Bulletin of Mathematical Biology, Vol. 59, No. 4, pp. 763–785, 1997
Elsevier Science Inc.

0092-8240/97 $17.00 + 0.00

S0092-8240(97)00038-4

UNDERSTANDING DRUG RESISTANCE FOR MONOTHERAPY TREATMENT OF HIV INFECTION

■ DENISE E. KIRSCHNER
Department of Microbiology and Immunology,
University of Michigan Medical School,
Ann Arbor, MI 48109-0620, U.S.A.
(*E.mail*: *kirschne@malthus.micro.med.umich.edu*)

■ G. F. WEBB
Department of Mathematics,
Vanderbilt University,
Nashville, TN 37240, U.S.A.
(*E.mail*: *webbgf00@ctrvax.vanderbilt.edu*)

The purpose of this study was to investigate strategies in the monotherapy treatment of HIV infection in the presence of drug-resistant (mutant) strains. A mathematical system is developed to model resistance in HIV chemotherapy. It includes the key players in the immune response to HIV infection: virus and both uninfected $CD4^+$ and infected $CD4^-$ T-cell populations. We model the latent and progressive stages of the disease, and then introduce monotherapy treatment. The model is a system of differential equations describing the interaction of two distinct classes of HIV—drug-sensitive (wild type) and drug-resistant (mutant)—with lymphocytes in the peripheral blood. We then introduce chemotherapy effects. In the absence of treatment, the model produces the three types of qualitative clinical behavior—an *uninfected steady state*, an *infected steady state* (latency), and *progression to AIDS*. Simulation of treatment is provided for monotherapy, during the *progression to AIDS* state, in the consideration of resistance effects. Treatment benefit is based on an increase or retention in $CD4^+$ T-cell counts together with a low viral titer. We explore the following treatment approaches: an antiviral drug which reduces viral infectivity that is administered early—when the $CD4^+$ T-cell count is $\geqslant 300/mm^3$, and late—when the $CD4^+$ T-cell count is less than $300/mm^3$. We compare all results with data. When treatment is initiated during the progression to AIDS state, treatment prevents T-cell collapse, but gradually loses effectiveness due to drug resistance. We hypothesize that it is the careful balance of mutant and wild-type HIV strains which provides the greatest prolonged benefit from treatment. This is best achieved when treatment is initiated when the $CD4^+$ T-cell counts are greater than $250/mm^3$, but less than $400/mm^3$ in this model (i.e. not too early, not too late). These results are supported by clinical data. The work is novel in that it is the first model to accurately simulate data before, during and after monotherapy treatment. Our model also provides insight into recent clinical results, as well as suggests plausible guidelines for clinical testing in the monotherapy of HIV infection.

1. Introduction. The problem of drug resistance in the treatment of HIV (human immunodeficiency virus) infection has become an increasingly significant barrier in the effectiveness of AIDS chemotherapy. Despite the initial success of monotherapy for HIV infection with agents such as AZT (Zidovudine), the benefits are short lived. A key factor in HIV chemotherapy failure is the rapid selection by HIV for drug-resistant (mutant) strains. It is observed that resistance develops rapidly to reverse transcription inhibitors such as AZT and other drugs that reduce viral production. This resistance is due to the ability of the virus to mutate and circumvent the normal transcription pathway which the chemotherapy interrupts (Volberding *et al.*, 1990). This resistance, together with side effects and toxicity, imposes time constraints on duration of treatment, as well as questions relating to timing and initiation of treatment. As monotherapy is still the common therapeutic approach in HIV infection in most clinics, and data are readily available, we study this as a first step in better understanding chemotherapy of HIV as a whole. Hence, in this study, we examine single-drug treatments (monotherapy) with those drugs that reduce viral infectivity (e.g. AZT, DDI, etc.). Present work of the authors involves the study of multidrug therapies as well as other immunotherapies and antiretroviral agents (such as protease inhibitors), both alone and in conjunction with these reverse transcriptase inhibition agents (Kirschner and Webb, 1997a, b).

There have been several earlier studies of monotherapy of HIV infection (McLean and Nowak, 1992; McLean *et al.*, 1991; Kirschner and Webb, 1996a). Previously (McLean and Nowak, 1992), it was conjectured that it was not the resistant strains which caused the large increase in viral load after long-term chemotherapy, but the growing supply of uninfected T cells. In other work (McLean *et al.* 1991), it was conjectured that the increase was due to nonlinear interactions of the virus and T-cell populations. Based on recent clinical evidence (e.g. Mohri *et al.*, 1993), it is now known that early resistance development is the primary reason for monotherapy failure. Previous work (Kirschner and Webb, 1996) presented a mathematical model which explored these issues of HIV treatment with chemotherapy in the absence of resistance constraints. This paper serves to extend that work to include resistance effects. Of interest here are the comparisons between monotherapy strategies administered early—when the $CD4^+$ T-cell count is $\geqslant 300/mm^3$, and late—when the $CD4^+$ T-cell count is less than $300/mm^3$. We study each of these chemotherapy approaches, in the presence of drug resistance, through a mathematical model, and then compare the results with clinical data. Our goals are to provide insight into recent clinical findings, and to learn something from the qualitative behavior of the models in these scenarios.

2. Methods

2.1. *The model.* To model the interaction of the immune system with HIV in the peripheral blood, we consider the group of white blood cells (lymphocytes) which have the protein marker CD4 ($CD4^+$ T cells) (the cells which become infected with HIV). The model considers both the non-infected (T) and infected (T^i) $CD4^+$ T cells. The infected class is then broken into two subclasses: those T cells which are infected with a drug-sensitive strain of HIV (T^s), and those cells which are infected with a drug-resistant strain of HIV (T^r). (Hence, the total infected T-cell population is $T^i = T^r + T^s$.) A model considering two major classes of infected cells (latently infected and actively infected) was considered earlier (Perelson, 1989; Perelson *et al.*, 1993; Kirschner and Perelson, 1995). Since the qualitative behavior of the dynamics is similar when both classes of infected T cells are combined, we do so for ease of computation. Finally, the population of plasma virus (V) is included. As in the case of the infected T cells, we include two subclasses of virus: the drug-sensitive (wild-type) strain of HIV (V_s), and the drug-resistant (mutant) strain of HIV (V_r) (hence, $V = V_s + V_r$). The dynamics of these populations interacting in the single compartment of the peripheral blood are modeled. The model is thus based on only three components: T, T^i and V. We believe this is the minimum number necessary to accurately describe the dynamic process and to test the model against a large literature of data. A schematic diagram describing the events is found in Fig. 1.

We assume that the initial innoculum is free virus and not infected cells (however, the model is robust in either case). We also assume that the sensitive virus strain is initially transmitted and is also dominant (there is evidence that resistant strains can be transmitted, but it appears to be a rare event). The explanation of the terms in Fig. 1 is as follows. s represents the source of new T cells. This source can be from bone marrow, thymus, or general production. This is enhanced by proliferative production. μ represents a natural death term since T cells have a finite life span (the average of which is $(1/\mu)$). We allow for the infection of $CD4^+$ T cells by both sensitive (see the left half of Fig. 1) and resistant (see the right half of Fig. 1) strains of virus with constant rates of infectivity k_s, k_r, respectively. Newly produced virion are released by infected $CD4^+$ T cells in which an average of N particles are released per infected cell (this idea was introduced in Perelson, 1989). We also use an earlier assumption (McLean and Nowak, 1992) that, upon each replication, there is a probability of $(1-q)$ that a significant mutation will take place, and that the proportion q remains faithful to the original strain. A *significant* mutation implies that a sensitive strain becomes resistant (or vice versa). T cells proliferate; hence, production of new virus takes place at rate qp, where p is the maximal

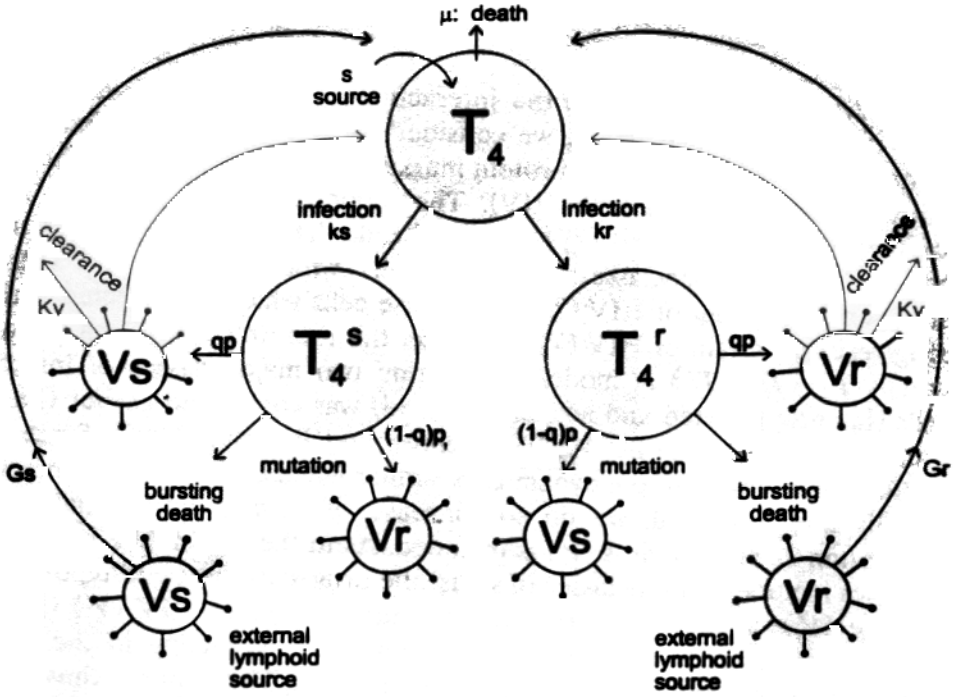

Figure 1. Schematic diagram of the interaction of virus with CD4$^+$ T cells. There are two virus populations: drug-sensitive HIV and drug-resistant HIV, and the respective infected T-cells (one group infected with drug-sensitive HIV, and the other with drug-resistant HIV) populations.

proliferation rate of the growth process; hence, production of mutated virus occurs at rate $(1-q)p$. Then, infected cells are lost either by having a finite life span, or through other immune clearance mechanisms. There is also a general clearance of virus at rate k_T.

As there is much evidence to support the major production of virus taking place in the external lymphoid system (LS), we account for this phenomenon as a major contributor of virions, other than the small amount produced in the blood (Lafeuillade *et al.*, 1996; Pantaleo *et al.*, 1996). The growth rates of these processes are $g_s(t)$ and $g_r(t)$, for the sensitive and resistant viral strains, respectively. We assume that there is a competitive advantage to the sensitive strain so that $g_r(t)$ is slightly less than $g_s(t)$. We do not attempt, however, to directly model a two-compartment system. so we treat this term as a rate of viral input (which we assume is parallel to what takes place in the blood (Lafeuillade *et al.*, 1996)). This model describes a generalized interaction between the immune system and HIV.

We choose differential equations as our medium to describe these interactions. This assumes that the infection is past the initial transient phase, and that there are large numbers in each of the populations, thus removing the need for any stochasticity (see Appendix a).

2.2. *Monotherapy.* In the absence of any chemotherapy, we assume that the sensitive strain of virus is dominant; but in the presence of treatment, selection is for resistance strains. Because of the development of resistance and side effects during single-drug chemotherapy, the time frame for which the drug can be administered is finite, and usually, less that two years (McLeod and Hammer, 1992; Volberding *et al.*, 1994). We model this phenomenon by treating for a 52-week window during the course of infection. We simulate the total $CD4^+$ T-cell population over time together with HIV levels as indicators of drug effectiveness. To include monotherapy in the model, it is necessary to mathematically mimic the effects of a drug which is a reverse transcriptase inhibitor. Such drugs reduce viral infectivity since they do not allow the viral DNA to be inserted into the host genome. Since multiple virions may infect a cell, such drugs may inhibit one virus, but allow another to get through or around the drug barrier. We therefore model treatment by inhibiting the infectivity of the virus. This would affect both the viral infectivity of new T cells, and also reduce the number of infectious virus from the LS. We achieve this by multiplying the parameters k_s and g_s in the model by functions which are "off" outside the treatment period (thus having no effect) and "on" during the treatment period (thus reducing viral infectivity). Treatment functions which achieve this are of the form

$$\begin{Bmatrix} 1 & \text{outside the treatment period} \\ P_1 & \text{during the treatment period} \end{Bmatrix}$$

where P_1 is the treatment effectiveness, $0 < P_1 < 1$. If $P_1 = 1$, there is no treatment effectiveness; if $P_1 = 0$, there is no viral production. A similar function, with treatment parameter P_2, is also applied to the external LS: however, it has less effect (i.e. $P_1 < P_2$ since it is a proportionate reduction) as we assume that the drug effectiveness is less in the LS (Lafeuillade *et al.*, 1996). Drugs such as AZT reduce viral activity in a dose-dependent manner. The efficacy of the chemotherapy may differ from patient to patient; therefore, P_i for $i \in \{1,2\}$ represents the varying effectiveness of the drug in halting viral activity in a given patient. (Note: our intention here is not to model the pharmokinetics, but only how treatment with viral infectivity inhibitors affects the dynamics of these populations.)

2.3. *Parameter estimates and turnover rates.* In selecting parameter values for our model, we were guided by T-cell and viral counts, life spans, lymph system dynamics, and turnover rates reported in clinical data. Essential considerations from clinical data (Ho *et al.*, 1995; Coffin, 1995; Perelson *et al.*, 1996) are high and rapid turnover rates of T cells and virus in the periphery and measured $CD4^+$ T-cell and virus totals during the course of HIV infection. Also, recent studies on the lymph system's contribution to

infection dynamics are incorporated (Lafeuillade *et al.*, 1996; Haase *et al.*, 1996).

2.3.1. *T-cell dynamics.* T cells typically decrease from 1000 to 0/mm^3 during the course of infection. In the blood, it has been estimated that an average of 3.5×10^7 are produced per day; when scaling by the blood volume (5×10^6), this yields the turnover of T cells to be 7/day/mm^3 (Ho *et al.*, 1995) and 8/day/mm^3 (Wei *et al.*, 1995). In our model, T-cell turnover changes slowly over the course of infection. A typical value is 11/day/mm^3 when the T-cell count is 300 per mm^3.

Since the T-cell population changes gradually during the course of infection, the production of T cells during short time intervals must be balanced by a loss of T cells due to infection and death. We are thus able to determine the T-cell equation kinetic parameters based upon the known T-cell counts and turnover rates. We calculate a death rate for uninfected T cells to be approximately 0.01/day, a proliferation rate of 0.05/day, and a viral infection rate of 2.5×10^{-4}. According to earlier work (Embretson *et al.*, 1993), approximately 5% of T cells are infected, and infected T cells have a life span of one–two days. We therefore calculate the death rate of infected T cells to be 0.5/day (this agrees with Perelson *et al.*, 1996). Stimulation and production of virus cause a clearance and extra loss of infected cells, and this infected cell clearance rate is also estimated to be 0.5/day.

2.3.2. *Virus dynamics.* From previous work (Ho *et al.*, 1995; Perelson *et al.*, 1996), it is estimated that the periphery viral levels ranged from 10 to 500/mm^3. Total body rates of viral turnover were also estimated, ranging from 6.8×10^8 to 1.03×10^{10}. Again, scaling by the blood volume, the peripheral viral turnover rates range from 100 to 2000/day/mm^3. In our model, virus turnover rates also change over the course of infection. A typical value is 300/day/mm^3 when the viral population is 100/mm^3. We assume that during steady state, viral production must be balanced by the viral clearance. Viral clearance was estimated (Perelson *et al.*, 1996) to be on average 3.07/day. In this study, viral contributions come from two sources: the lymph system virus and plasma virus. Viral production in the periphery is estimated in the model to be on the order of 10 virions/CD4$^+$ T cell. This estimate agrees with data recently presented (Levy *et al.*, 1996). In the model, the source of virus from the LS accounts for more than 90% of virus production in the peripheral blood.

Table 1 provides a summary of T-cell and virus lifespans and turnover rates from both computed model output values and from clinically reported values. The model values and the reported values are in notably close agreement.

Table 1. Predictive vs. clinical rate data

Rate information	Model values[a]	Clinical data values
$CD4^+$ T-cell turnover in the blood		7/day (Ho *et al.*, 1995) 8/day (Wei *et al.*, 1996)
Plasma virus turnover		136/day (Ho *et al.*, 1995) 2060/day (Perelson *et al.*, 1996)
Infected $CD4^+$ T-cell life span	1.5 days	Less than 1 or 2 days (Coffin, 1995)
Viral production per T cell	10 virions/cell	30–100 virions/cell (Levy *et al.*, 1996)
Uninfected $CD4^+$ T-cell life span	29 days (in HIV) 100 days (no disease)	No data avail.; est. to be 1 year (McLean *et al.*, 1991)
Percent of $CD4^+$ T cells infected	4%	5% of total (Embretson *et al.*, 1993)
Virus life span	0.33 days	0.3 days (Perelson)
Percent of virus in the blood produced in the blood	7%	No data available

[a]Model values are computed for $T(t) = 300/\text{mm}^3$ and $V(t) = 100/\text{mm}^3$. Other choices for $(T(t), V(t))$ give similar values.

3. Results.

3.1. *Results without chemotherapy.* To begin numerical studies, first examine the model in the absence of infection. With no HIV present in the system, the model settles into an *uninfected steady state* (Fig. 2A). Second, examine the model in the presence of HIV, but in the absence of any treatment. Two different numerical solutions are given in Fig. 2 (B and C). Figure 2B represent individuals who are non-progressors during the latent stage of the disease, when the T-cell counts and viral titers are approximately constant. The third stage, *progression to AIDS*, represents individuals who are now progressors. The viral titers begin to grow, and the CD4 T-cell counts drop to very low levels. The assumption that the wild-type strain is dominant in the absence of drug pressure can be seen when comparing the two viral population graphs in Fig. 2C. The different results are obtained by varying the external lymphoid input rates of virus. Since the majority of viral production takes place outside the periphery in the lymphoid system, it is plausible that the external lymphoid system input rates could control the disease progression (Pantaleo *et al.*, 1993; Lafeuillade *et al.*, 1996). It is during this disease state that we examine the effects of chemotherapy. To compare with data, Fig. 2D shows the T-cell counts over time for a typical patient never receiving treatment (Redfield and Burke, 1988).

Panel 2A

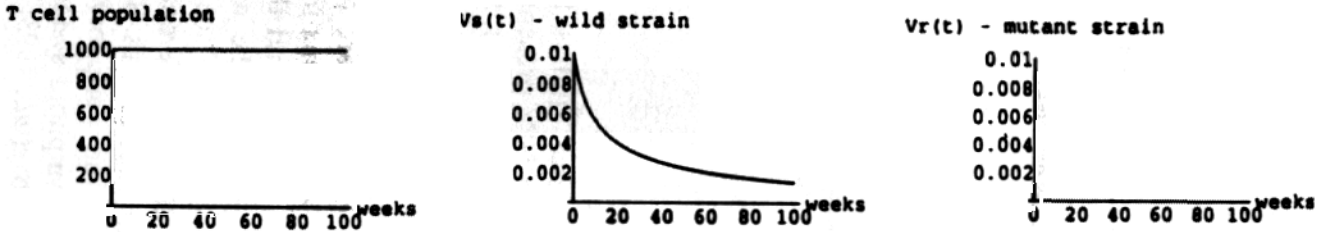

Panel 2B

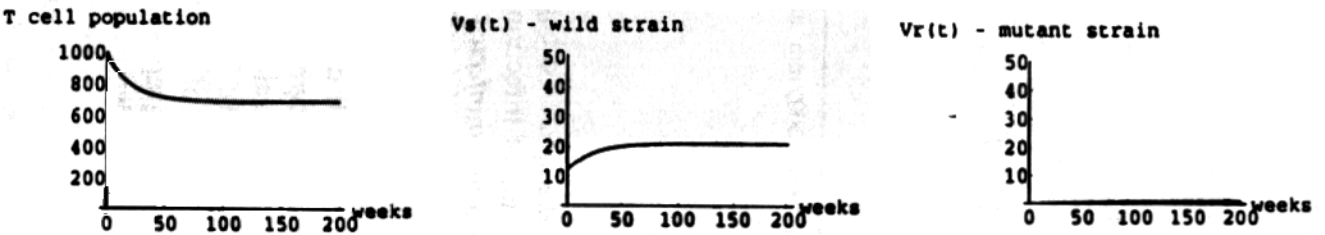

Panel 2C

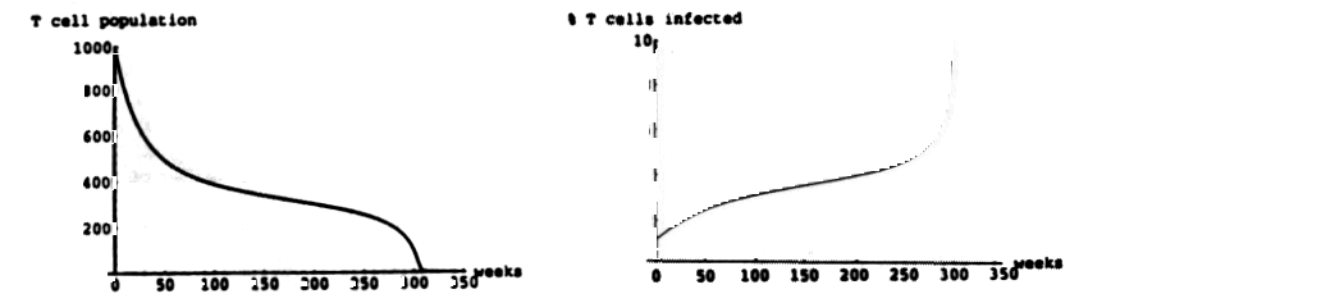

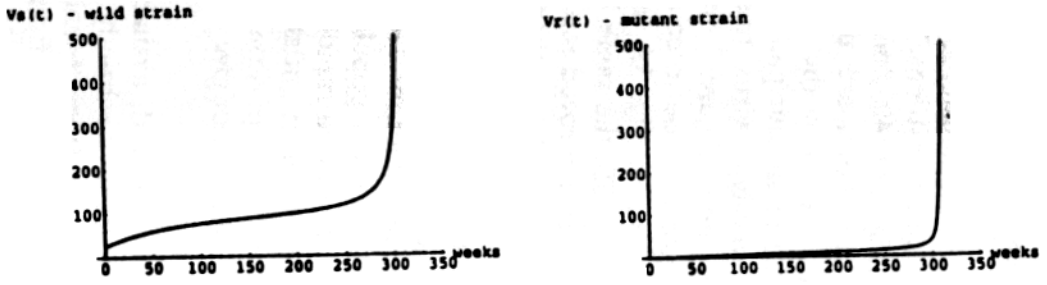

Panel 2D

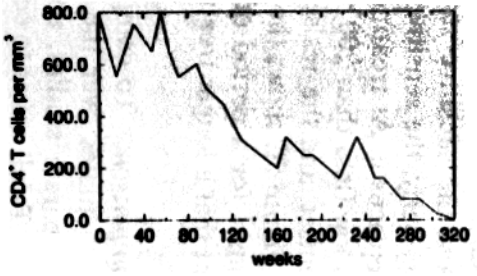

Figure 2. Numerical solutions to the model with time in weeks. Panel A is the *uninfected steady state* with a low LS viral input, and panel B is the *infected steady state* (latency) with a medium LS viral input. Panel C represents the *Progression to AIDS* state with a high viral input. Four figures are presented in panel C: the T-cell population, the percent infected T cells, the two viral populations—drug sensitive (wild type) and drug resistant (mutant). Panel D shows the T-cell counts for a typical patient over time (Redfield and Burke, 1988).

3.2. *Chemotherapy results.* The simulations of chemotherapy we provide explore many issues relating to the different techniques of administering chemotherapy to an HIV-infected individual. We focus on the issues of when to initiate treatment and when treatment loses effectiveness. The presence of resistance plays a vital role in consideration of these issues. Our treatment simulations are based upon typical reported clinical results with AZT (see Figs. 6 and 7). The treatment parameters $P_1 = 0.9$ and $P_2 = 0.99$ (as discussed above) give model output concordant with the graphs in Figs. 6 and 7.

We first define two disease-treatment stages: *early*—when $CD4^+$ T cells are above $300/mm^3$, and *late*—when $CD4^+$ T cells are below $300/mm^3$. Figures 3 and 4 represent typical AZT treatment administered for 52 weeks (shaded regions) at four different treatment initiation times. T-cell counts at initiation of treatment were $500/mm^3$ (Fig. 3A), $400/mm^3$ (Fig. 3B), $300/mm^3$ (Fig. 4A), and $200/mm^3$ (Fig. 4B). Shown are the effects of treatment on T-cell counts (solid line) together with the no-treatment (hashed line) case for comparisons. Presented in all four panels are T-cell counts, change in T-cell counts, plasma wild-type virus titers, plasma mutant virus titers, and total plasma viral titers. Figure 5 represents a composite of nine different initiation scenarios for ease in comparing the results. Notice how the increased T-cell counts in Fig. 5A are maximal when treatment is initiated at $300/mm^3$. In Fig. 5B, the same is also true. These results indicate the following: there is an improved result as treatment initiation values for T cells counts go from high (larger than $500/mm^3$) to around middle ($300/mm^3$). This is due to the fact that the resistant strain is low, and the sensitive strain is also low after treatment. If the treatment is very early, the sensitive strain is extinguished, but the resistant strain rapidly replaces it. As treatment initiation values for T-cell counts go from middle to low (less than $200/mm^3$), the resistant population is much higher at the outset, and the resistant strain can again rapidly replace the sensitive virus. Figure 5C shows the results of treatment initiated at a T-cell count of $300/mm^3$ for a period of two years. A comparison with Fig. 3A makes it evident that a longer treatment period does not give better results.

3.3. *Data comparison.* To compare our results with available data, we have chosen key studies over the past five years. We briefly present the results of the separate studies, and present data (Figs. 6 and 7) on the changes in $CD4^+$ T-cell count to compare with our results (from Figs. 3–5).

Study 1 (Hamilton *et al.*, 1992). This is a study of early versus late AZT treatment in symptomatic HIV patients. Patients with $CD4^+$ T-cell counts between 200 and $500/mm^3$ (early-solid line, Fig. 6C) were compared with patients who had T-cell counts below $200/mm^3$ (late-hashed line, Fig. 6C). Results indicated much less

benefit to patients starting treatment with counts below $200/mm^3$.

Study 2 (Fischl *et al.*, 1990). This study treated patients with CD4 T-cell counts between 200/ and $500/mm^3$. Either a placebo (hashed lines, Figs. 6A, 7C) or AZT (solid lines, Figs. 6A, 7C) were administered for 52 weeks.

Study 3 (Concorde Coordinating Committee, 1994). Patients in this study were given *immediate* (hashed line, Fig. 6B) AZT treatment versus *deferred treatment* (solid line, Fig. 6B), that is, they were given a placebo until persistently low T-cell counts or until ARC or AIDS onset, and then were given AZT. In this study, treatment was not recommended for symptom-free patients.

Study 4 (Vella *et al.*, 1994). This study treated patients with CD4 T-cell counts between 200 and $500/mm^3$, with a mean CD4 T-cell count of $308/mm^3$. Results indicate that the effects of AZT on non-progressors cannot be sustained for more than 70 weeks (Fig. 6D).

Study 5 (Ruffault *et al.*, 1995). The authors study the prognostic value of plasma viremia under AZT treatment. They categorize patients into the two groups of progressors (light lines, Fig. 7A, B) and non-progressors (dark lines Fig. 7A, B). They claim a strong correlation between virus titers and clinical outcomes.

Study 6 (Loveday *et al.*, 1995). The authors studied 11 patients whose $CD4^+$ T-cell counts were all at or below $320/mm^3$. The study implied that there were several phases of AZT action (Fig. 7D): the "early fall phase" is the time of maximal drug efficacy; the "return-to-baseline phase" is independent of resistance; the "plateau phase" where, over a period of months, the viral titer slowly rises due to resistance; and finally, "the rebound-to-baseline phase" when AZT is stopped and viral titer recovers.

The above studies can be used to compare our results with the clinical data.

Early treatment (CD4 T-cell treatment initiation value $> 300/mm^3$). The Concorde study indicates no benefit to patients with CD4 T-cell counts $> 500/mm^3$ (Fig. 6B, hashed line), as do the model simulations (Fig. 5A). The model simulations indicate an improved benefit as starting values decrease from 500 to $300/mm^3$.

Late treatment (CD4 T-cell treatment initiation value $< 300/mm^3$). The clinical data in Fig. 6C (hashed) and Fig. 7A, B (solid line) indicate little benefit to patients starting treatment with CD4 T-cell counts $< 200/mm^3$, as do the model simulations (Fig. 5B). The model simulations indicate a decreased benefit as treatment starting values decrease from 300 to $200/mm^3$.

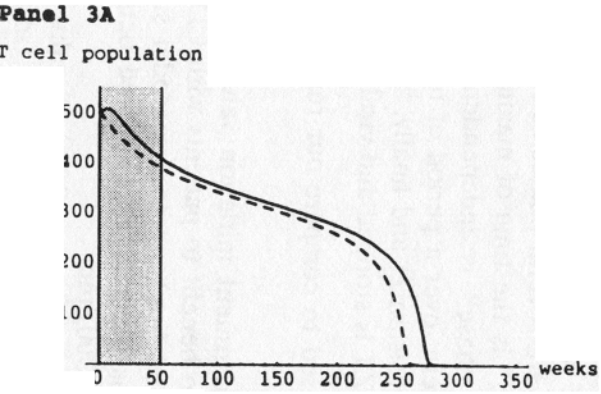
Panel 3A
T cell population
500
400
300
200
100
0 50 100 150 200 250 300 350
weeks

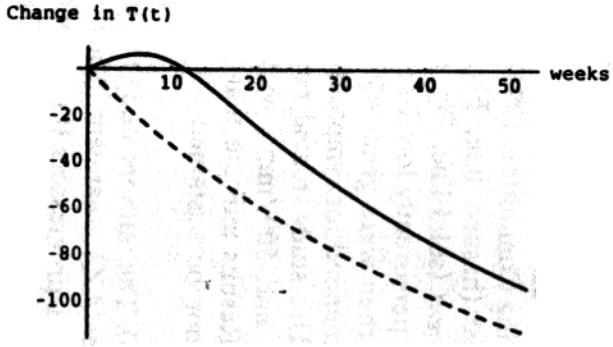
Change in T(t)
10 20 30 40 50
weeks
-20
-40
-60
-80
-100

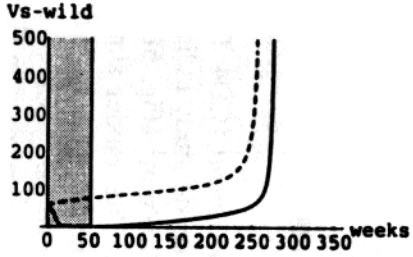
Vs-wild
500
400
300
200
100
0 50 100 150 200 250 300 350
weeks

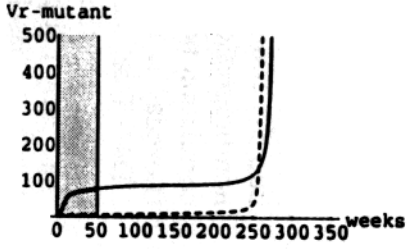
Vr-mutant
500
400
300
200
100
0 50 100 150 200 250 300 350
weeks

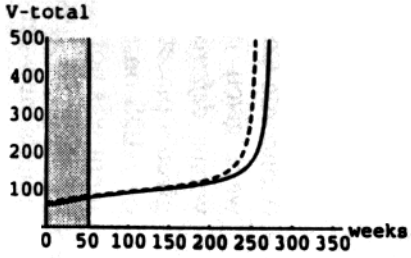
V-total
500
400
300
200
100
0 50 100 150 200 250 300 350
weeks

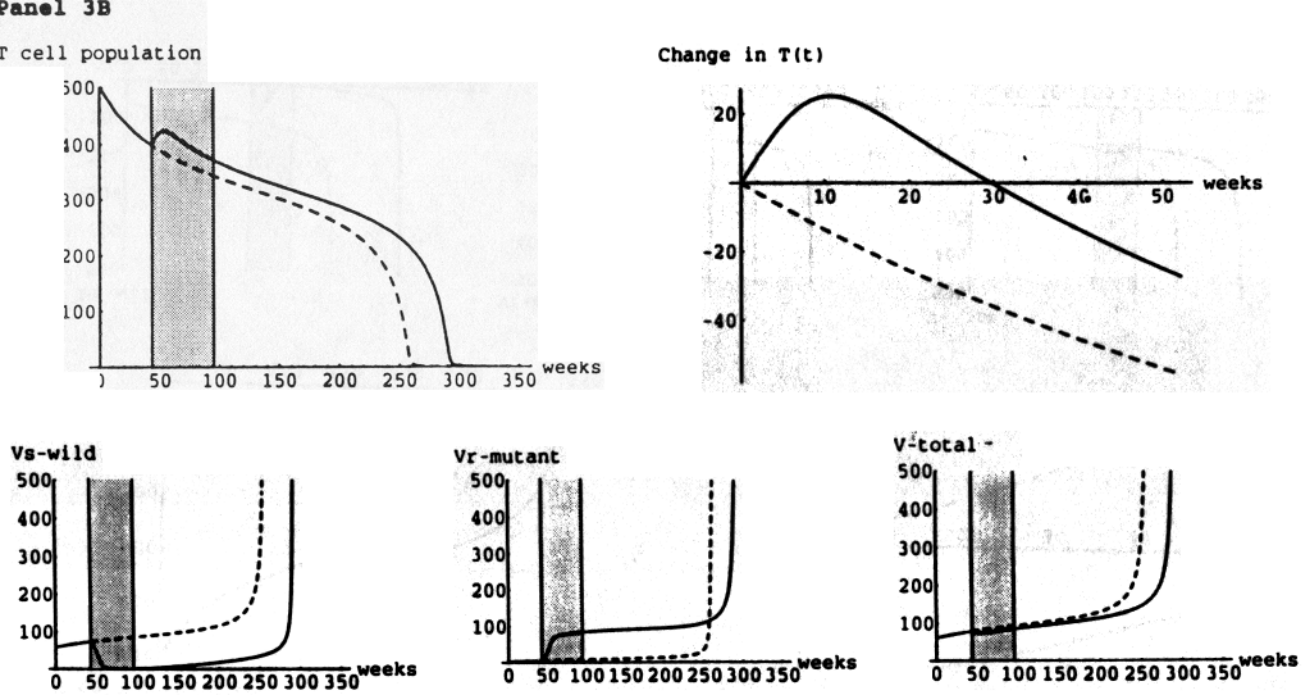

Figure 3. Numerical solutions to the model during therapy. All treatment was carried out during the progression to AIDS for one year (52 weeks). Numerical results are given for the administration of treatment (shaded regions) at two different treatment initiation times: T-cell counts initially 500/mm^3 (panel A) and T-cell counts initially 400/mm^3 (panel B). Shown are the effects of treatment on T-cell counts together with the no-treatment case (hashed lines) for comparisons. Presented in both panels are: T-cell counts, change in T-cell counts, wild-type virus titers, mutant virus titers, and total plasma viremia.

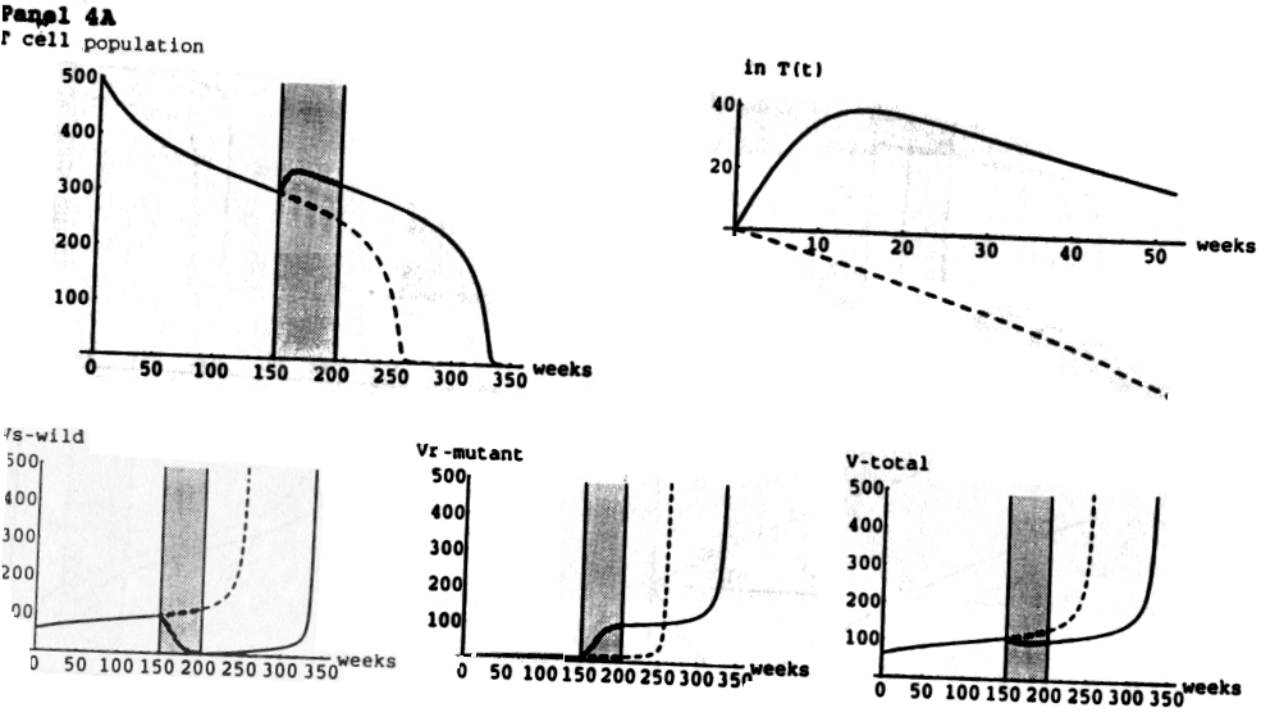
Panel 4A
T cell population
500
400
300
200
100
0 50 100 150 200 250 300 350 weeks
in T(t)
40
20
10 20 30 40 50 weeks
Vs-wild
500
400
300
200
100
0 50 100 150 200 250 300 350 weeks
Vr -mutant
500
400
300
200
100
0 50 100 150 200 250 300 350 weeks
V-total
500
400
300
200
100
0 50 100 150 200 250 300 350 weeks

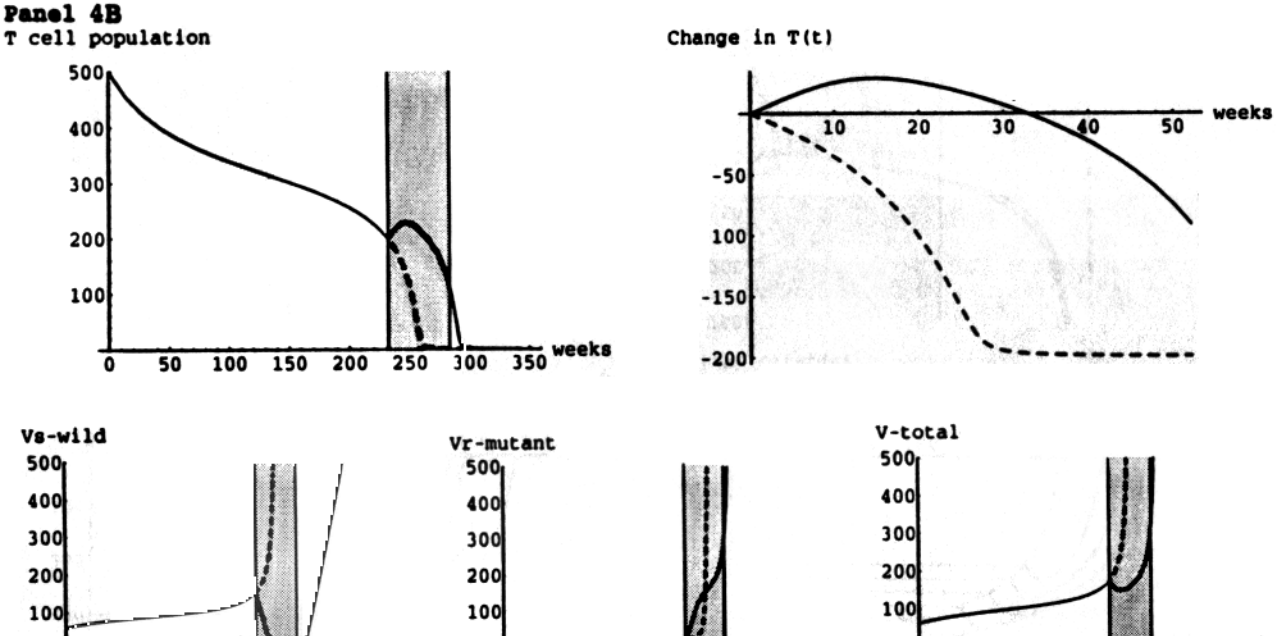

Figure 4. Numerical solutions to the during therapy as in Fig. 3, but with T-cell count initially at 300/mm^3 (panel A) and 200/mm (panel B).

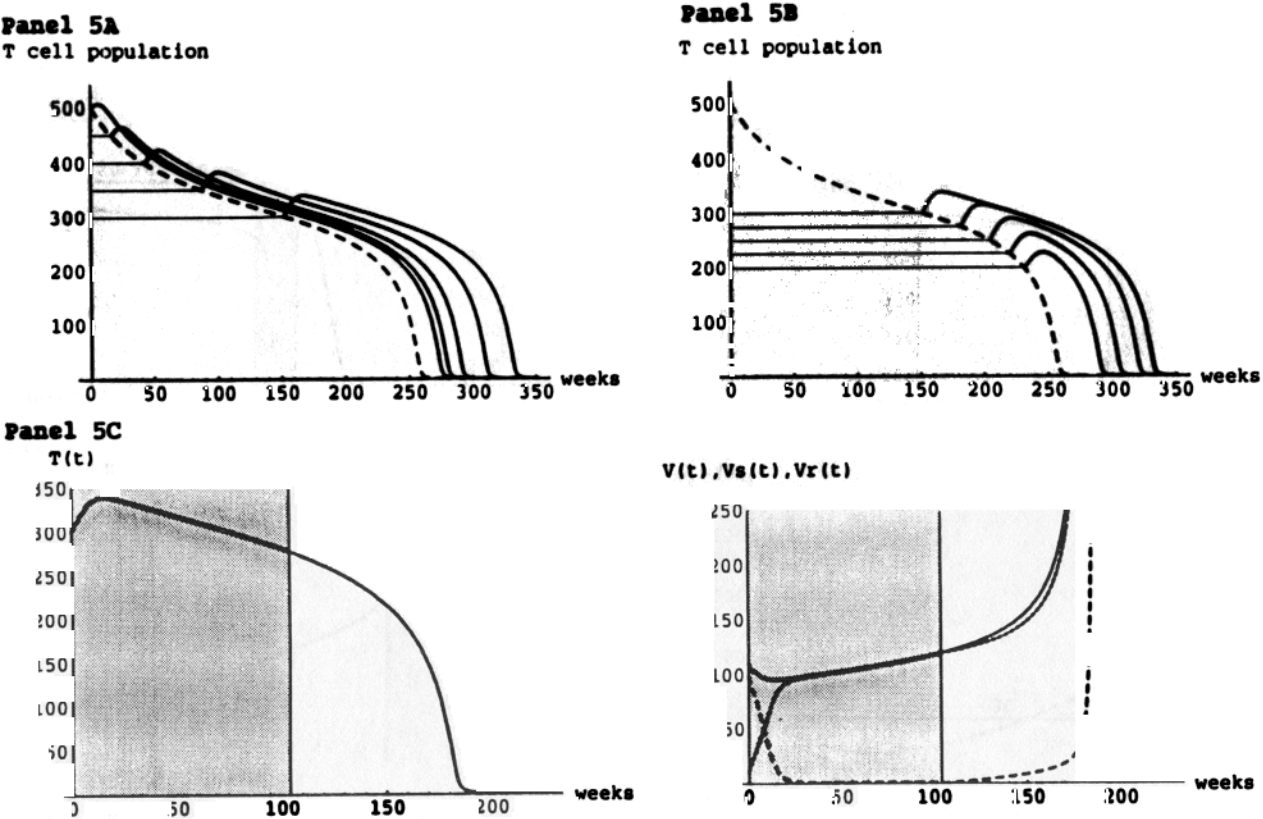

Figure 5. Composite of nine different initiation scenarios (from Figs. 3 and 4) for ease of comparing the results. The hashed line indicates the results without treatment. Notice how the increased T-cell counts and long-term survivability in panel A are maximal when treatment is initiated at $300/mm^3$. In panel B, the same is also true. Panel C shows the results of treatment initiated at T-cell count of $300/mm^3$ for a period of two years. When compared with Fig. 4, panel A, it may be seen that there is no additional benefit to treatment for two years as compared to treatment for one year.

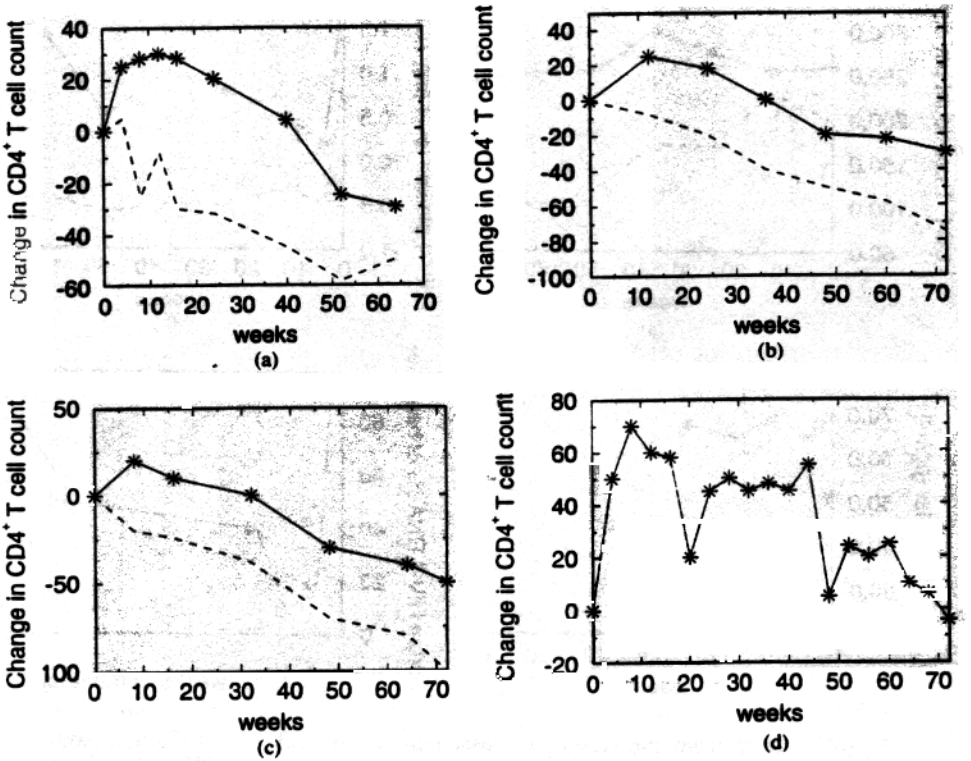

Figure 6. Data from the studies discussed in section 3.3, "Data Comparison." Panel A is data from (Fischl *et al.*, 1990). This study treated patients with CD4 T-cell counts between 200 and 500/mm^3. Either a placebo (hashed line) or AZT (solid line) was administered for 52 weeks. Panel B is data from earlier work (Concorde Coordinating Committee, 1994). Patients in this study were given *immediate* (hashed line) AZT treatment versus *deferred* (solid line) placebo until persistently low T-cell counts or until ARC or AIDS onset, and then AZT. The immediate treatment group included patients with CD4 counts > 500. This study did not recommend treatment in symptom-free patients. Panel C is data from previous work (Hamilton *et al.*, 1992). This is a study of early versus late AZT in symptomatic HIV patients. Patients with CD4 T-cell counts between 200 and 500/mm^3 (solid line) were compared with patients who had T-cell counts below 200/mm^3 (hashed line). Results indicated a delay to progression to AIDS in the first group. Panel D is data from earlier work (Vella *et al.*, 1994). This study treated patients with CD4 T-cell counts between 200 and 500/mm^3, with a mean CD4 T-cell count of 308/mm^3. Results indicate that the effects of AZT on non-progressors cannot be sustained for more than 70 weeks.

Middle treatment (CD4 T-cell treatment initiation value near 300/mm^3). The clinical data for treatment initiation in a middle range (Fig. 6A–C) indicate an average increase of 30–60 counts in the CD4 T-cell levels. This peaks about week 10 after treatment initiation, and returns to baseline after 40–60 weeks. The model simulations (Figs. 4A, 5A, 5B) give this same qualitative behavior. The viral counts compare extremely

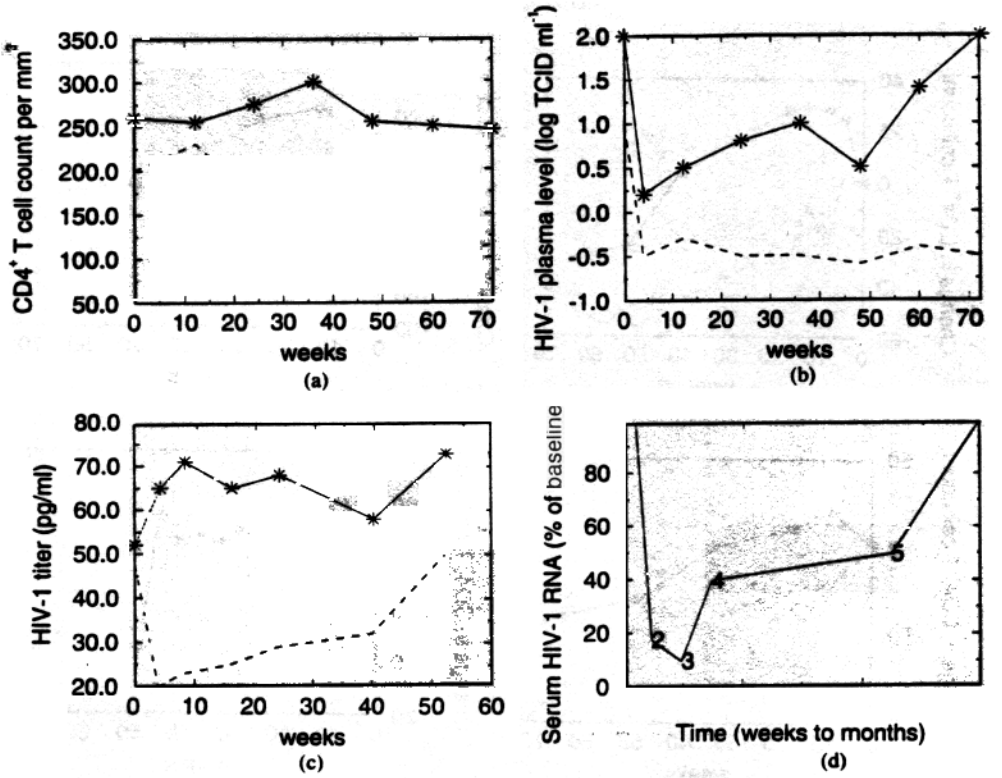

Figure 7. Data from the studies discussed in section 3.3, "Data Comparison." Panels A and B are data from earlier work (Ruffault *et al.*, 1995). They study the prognostic value of plasma viremia under AZT treatment. They categorize patients into the two groups of progressors (dark lines) and non-progressors (light lines). They claim a strong correlation between virus titers and clinical outcomes. Panel C is data from previous work (Fischl *et al.*, 1990). This study treated patients with CD4 T-cell counts between 200 and 500/mm^3. Either a placebo (hashed line) or AZT (solid line) was administered for 52 weeks. Panel D is a schematic from other work (Loveday *et al.*, 1995). This study defined phases of AZT treatment as: the "early fall phase (2–3)" is the time of maximal drug efficacy, the "return-to-baseline phase (3–4)" is independent of resistance, the "plateau phase (4–5)" where, over a period of months, the Viral titer slowly rises due to resistance, and finally, "the rebound-to-baseline phase (5–on)" when AZT is stopped and viral titer recovers.

well with Fig. 7D, the phase model of monotherapy (Loveday *et al.*, 1995).

These comparisons indicate that the model can qualitatively predict and depict clinical trial outcomes. The model thus can be used to explain the results which are seen in both the model simulations and the clinical trials. The model simulations indicate that the balance of the resistant and sensitive strains of plasma viremia levels is the major factor in understanding the success or failure of treatment. When treatment is administered too

early, the sensitive strain is greatly inhibited (see data comparison in Fig. 7); however, the resistant strain now can take off with no competition (Larder *et al.*, 1989; Mohri *et al.*, 1993; Richman *et al.*, 1990). If treatment is administered too late, the sensitive strain has had a chance to reach higher levels, and even though it is reduced upon initiation of treatment, the mutant strain can now rapidly recover the high viral level. In either case, the total viremia is high. When treatment is administered during an intermediate case, total viral level remains lowest (see Fig. 3).

4. Discussion. The goals of this study were to create a mathematical model which described the interaction of the immune system with HIV, and to use this model to explore chemotherapy treatments in the presence of resistant viral strains. The model was constructed with parameters based on recent clinical data on HIV dynamics. The model was used to simulate a variety of possible treatment regimes and outcomes. These simulations revealed that the greatest benefits to T-cell counts and long-term survivability occur when treatment is initiated at an intermediate T-cell count (approximately $300/mm^3$). Treatment initiation at T-cell counts higher than $500/mm^3$ or lower than $200/mm^3$ provided much less benefit. It has been shown that initiation of treatment at lower T-cell counts is associated with accelerated development of resistance. This is corroborated in our simulations wherein treatment initiated after T cells drop below $200/mm^3$ has almost no long-term benefit. In our simulations, the optimal time for initiation of treatment occurs when viral titers are still relatively low, particularly for drug-resistant strains. If, however, treatment is initiated too early, drug-resistant viral strains rapidly replace drug-sensitive strains, and the benefits of treatment are wasted. Our model reveals that the benefits of treatment depend upon the balance between sensitive and resistant viral strains. Since they are in competition, suppression of the sensitive strain during treatment allows the resistant strain to flourish. Treatment that continues past the time of complete replacement of sensitive by resistant virus gives little added benefit. It is the relative proportion of sensitive and resistant virus that determines the outcome of treatments. Our model indicates that strategies which take this into account can improve treatment effectiveness.

Finally, we are now working on a two-compartmental model to more accurately understand the role of the blood and lymph system interactions in overall HIV dynamics. Recent clinical advances in lymphoid studies are facilitating this goal.

The authors are grateful to M. Cloyd, S. Raffanti, J. Richardson and B. Graham for helpful discussions. They also thank the reviewers for constructive comments. This work was supported under Grants DMS 9596073 and DMS 9202550 from the National Science Foundation.

APPENDIX

This is the presentation of the model. Define $T(t)$ to be the uninfected CD4$^+$ T-cell population, $T^s(t)$ to be the population of T cells infected with wild-type virus, $T^r(t)$ to be the population of T cells infected with mutant virus, $V_s(t)$ to be the wild-type viral load, and $V_r(t)$ to be the mutant viral load.

$$\frac{dT(t)}{dt} = s(t) + p(t)T(t) - \mu_T T(t) - \mathbf{P}_1 k_s T(t) V_s(t) - k_r T(t) V_r(t)$$

$$\frac{dT^s(t)}{dt} = k_s T(t) V_s(t) - \mu_{T_i^s} T^s(t) - p_i^s(t) T^s(t)$$

$$\frac{dT^r(t)}{dt} = k_r T(t) V_r(t) - \mu_{T_i^r} T^r(t) - p_i^r(t) T^r(t) \tag{A3}$$

$$\frac{dV_s(t)}{dt} = q \cdot p_n^s(t) T^s(t) + (1-q) \cdot p_n^r(t) T^r(t) - k_T(t) V_s(t) + \mathbf{P}_2 g_s(t) \tag{A4}$$

$$\frac{dV_r(t)}{dt} = q \cdot p_n^r(t) T^r(t) + (1-q) \cdot p_n^s(t) T^s(t) - k_T(t) V_r(t) + g_r(t). \tag{A5}$$

Initial conditions are $T(0) = T_0$, $T^s(0) = 0$, $T^r(0) = 0$, $V_s(0) = V_{s0}$, $V_r(0) = 0$.[1]

The model is explained as follows. The terms of (A1), $s(t) - p(t)T(t)$, represent the source of new T cells. This incorporates T cells from the bone marrow, thymus and general production. It also includes proliferative production (whether direct or indirect) due to the presence of antigen. This production changes over the course of infection, which is accounted for in the time-dependent rates. This is followed by a natural death term because cells have a finite life span, the average of which is $(1/\mu_T)$. The last two terms represent the infection of CD4$^+$ T cells by both resistant and sensitive strains of virus. These terms are mass action type terms with constant rates of infectivity k_s, k_r. We assume that the law of mass action applies here based on the large numbers of cells and virion involved. P_1 represents the effects of treatment on viral infectivity in the plasma. Equations (A2) and (A3) describe changes in the infected population of CD4$^+$ T cells, T^s and T^r, respectively. (We assume that each T cell is dominated by, and hence producing, only one strain of the virus, either V_s or V_r.) The first gain terms for each carry over from the loss terms in (A1). Then, infected cells are lost by such processes as natural death, viral killing, apoptosis or homing to LS.

In (A4) and (A5), the first terms are the source for the virus population. Newly produced virion come from production by infected CD4$^+$ T cells (from (A2) and (A3)), in which new virion are produced at rates $p_n^s(t)$ and $p_n^r(t)$, respectively. We assume that, upon each replication, there is a probability of $(1-q)$ that a significant mutation will take place, and that the proportion q remains faithful to the original strain. (A *significant* mutation implies that either a wild type (sensitive) strain mutates to being resistant or vice versa.) This follows from earlier work (McLean and Nowak, 1992). The next term represents viral clearance (estimated in Perelson *et al.*, 1996).

As there is much evidence to support the major production of virus taking place in the external lymphoid system (LS), we account for this phenomenon as a major contributor of virions, other than the small amount produced in the blood (Lafeuillade *et al.*, 1996). The input rates of lymphoid system virus are $g_s(t)$ and $g_r(t)$ for the sensitive and resistant viral strains, respectively. They are time-dependent, as this will vary over the course of infection.

[1] If we assume that $k_s = k_r$ and sum the two equations for infected T cells ($T^i = T^r + T^s$) and similarly sum the viral equations ($V = V_s + V_r$), the equations reduce to that of the non-resistance model in (Kirschner and Webb, 1996).

Table 2. Variables and parameters

Parameters	Functional form	Interpretation	Value
	$10-(5V(t)/15+V(t))$	Source of uninfected T cells	$\text{mm}^3\ d^{-1}$
		Death rate of uninfected $CD4^+$ T-cell population	$0.01d^{-1}$
μ_{T^s}		Death rate of (T^s) infected $CD4^+$ T-cell population	$0.5d^{-1}$
μ_{T^r}		Death rate of (T^r) infected $CD4^+$ T-cell population	$0.5d^{-1}$
k_s		Rate $CD4^+$ T cells become infected by free virus, V_s	2.5×10^{-4} $\text{mm}^{-3}\ d^{-1}$
k_r		Rate $CD4^+$ T cells become infected by free virus, V_r	2.5×10^{-4} $\text{mm}^{-3}\ d^{-1}$
$k_T(t)$	$\cdot\ k_T T(t)$	Time-dependent rate of viral clearance	d^{-1}
k_T		Coefficient of viral clearance	$0.01\ \text{mm}^{-3}\ d^{-1}$
$p(t)$	$(pV(t)/C+V(t))$	Proliferation rate of the $CD4^+$ T-cell population	d^{-1}
p		Maximal proliferation	$0.05d^{-1}$
C		Half saturation constant of uninfected T-cell proliferation	$188\ \text{mm}^3$
$p_i^s(t)$	$(p_i^s V_s(t)/C_i+V(t))$	Rate of clearance of sensitively infected $CD4^+$ T cells	d^{-1}
p_i^s		Maximal clearance rate (sensitive)	$0.5d^{-1}$
p_i^r		Maximal clearance rate (resistant)	$0.5d^{-1}$
C_i		Half saturation constant	$188\ \text{mm}^3$
$p_i^r(t)$	$(p_i^r V_r(t)/C_i+V(t))$	Rate of clearance of resistant infected $CD4^+$ T cells	d^{-1}
$g_s(t)$	$(g_s V_s(t)/b+V(t))$	Input rate of lymphoid (drug-sensitive) virus	$\text{mm}^3\ d^{-1}$
g_s		Maximal input rate from LS	$330d^{-1}$
$g_r(t)$	$(g_r V_r(t)/b+V(t))$	Input rate of lymphoid (drug-resistant) virus	$\text{mm}^3\ d^{-1}$
g_r		Maximal input rate from LS	$(0.9995)(330)d^{-1}$
b		Half saturation constant of the lymphoid viral source	$8\ \text{mm}^3$
$p_n^s(t)$	$N\times p_i^s(t)$	Production rate of (sensitive) virus from plasma T-cell production	d^{-1}
$p_n^r(t)$	$N\times p_i^r(t)$	Production rate of (resistant) virus from plasma T-cell production	d^{-1}
$(1-q)$		Probability that a significant mutation will occur	0.001
P_1		Percentage effectiveness treatment (multiplying k_s)	0.9
P_2		Percentage effectiveness treatment (multiplying $g_s(t)$)	0.99
N		Number of free viruses produced per infected plasma T cell	10

P_2 represents the effects of treatment on viral infectivity in the LS. The model (A1)–(A5) describes the interaction of the immune system with HIV. The parameters and values are given in Table 2.[2]

[2] In the notation of Arden, the following are equivalent: $\delta_T=\mu_T$, $\beta=k_s$, $I=T^s$, $\delta=\mu_{T^s}$, $c\simeq -k_T(t)$, $p\simeq p_n^s(t)\simeq N\delta$.

REFERENCES

Coffin, J. M. 1995. HIV population dynamics in vivo: implications for genetic variation, pathogenesis and therapy. *Science* **267**, 483–489.

Concorde Coordinating Committee. 1994. MRC/ANRS randomized double-blind controlled trial of immediate and deferred AZT in symptom-free HIV infection. *The Lancet* **343**, 871–881.

Embretson, J. *et al.* 1993. Analysis of HIV infected tissues by amplification and *in situ* hybridization reveals latent and permissive infections at single-cell resolution. *Proc. Nat. Acad. Sci.* **90**, 357.

Fischl, M. A. *et al.* 1990. The safety and efficacy of AZT in the treatment of subjects with mildly symptomatic HIV type 1. *Annals Int. Med.* **112**, 727–737.

Hamilton, J. D. *et al.* 1992. A controlled trial of early vs. late treatment with AZT in symptomatic HIV infection. *New England J. Med.* **326**, 437–443.

Ho, D. D. *et al.* 1995. Rapid turnover of plasma virions and CD4 lymphocytes in HIV-1 infection. *Nature* **373**, 123–126.

Kirschner, D. and A. Perelson. 1995. A model for the immune system response to HIV: AZT treatment studies. In *Mathematical Populations Dynamics III. Theory of Epidemics*, O. Arino, D. Axelrod and M. Kimmel (Eds), Vol. 1, pp. 295–310. Winnepeg, Man., Canada: Wuerz.

Kirschner, D. and G. F. Webb. 1996. A model for treatment strategy in the chemotherapy of AIDS. *Bull. Math. Biol.* **58**, 367–391.

Kirschner, D. and G. F. Webb. 1997a. A mathematical model of combined drug therapy of HIV infection. *J. Theoret. Med.*, to appear.

Kirschner, D. and G. F. Webb. 1997b. Qualitative differences in HIV chemotherapy between resistance and remission outcomes. *Emerging Infect. Dis.*, to appear.

Lafeuillade, A., C. Poggi, N. Profizi *et al.* 1996. Human immunodeficiency virus type 1 in lymph nodes compared with plasma. *J. Infect. Dis.* **174**, 404–407.

Larder, B. A. *et al.* 1989. HIV with reduced sensitivity to zidovudine (AZT) isolated during prolonged therapy. *Science* **243**, 1731–1734.

Levy, J. A., J. Guthrie and T. Elbeik. 1996. Plasma viral load, $CD4^+$ cell counts, and HIV-1 production in cells. *Science* **271**, 670–671.

Loveday, C. *et al.* 1995. HIV-1 RNA serum-load and resistant viral genotypes during early zidovudine therapy. *LANCET* **345**, 820–824.

McLean, A. and M. Nowak. 1992. Competition between AZT sensitive and AZT resistant strains of HIV. *AIDS* **6**, 71–79.

McLean, A. *et al.* 1991. Population dynamics of HIV within an individual after treatment with AZT. *AIDS* **5**, 485–489.

McLean, A. R. and M. A. Nowak. 1992. Competition between zidovudine-sensitive and zidovudine-resistant strains of HIV. *AIDS* **6**, 71–79.

McLeod, G. X. and S. M. Hammer. 1992. Zidovudine: 5 years later. *Annals Int. Med.* **117**, 487–501.

Mohri, H. *et al.* 1993. Quantitation of zidovudine-resistant human immunodeficiency virus type 1 in the blood of treated and untreated patients. *Proc. Nat. Acad. Sci. USA* **90**, 25–29.

Pantaleo, G., C. Graziosi *et al.* 1996. HIV infection is active and pregressive in lymphoid tissue during the clinically latent stage of disease. *Nature* **362**, 355–358.

Perelson, A. *et al.* 1996. HIV-1 dynamics in vivo: clearance rate, infected cell lifespan, and viral generation time. *Science* **271**, 1582–1585.

Perelson, A. *et al.* 1993. The dynamics of HIV infection of $CD4^+$ T cells. *Math. Biosci.* **114**, 81–125.

Perelson, A. S. 1989. Modeling the interaction of the immune system with HIV. In *Mathematical and Statistical Approaches to AIDS Epidemiology, Lect. Notes in Biomath.*, C. Castillo-Chavez (Ed), Vol. 83, pp. 350–370. New York: Springer-Verlag.

Redfield, R. and D. Burke. 1988. HIV infection: the clinical picture. *Sci. Amer.* 90–98.

Richman, D. D. *et al.* 1990. Effect of stage of disease and drug dose on zidovudine susceptibilities of isolates of human immunodeficiency virus. *J. Acquired Immune Deficiency Syndromes* **3**, 743–746.

Ruffault, A. *et al.* 1995. The prognostic value of plasma viremia in HIV-infected patients under AXT treatment—a two-year follow-up study. *J. AIDS* **9**, 43–248.
Vella, S. *et al.* 1994. Long-term follow up of AZT therapy in asymptomatic HIV infection: results of a multicenter cohort study. *J. AIDS* **7**, 31–38.
Volberding, P. A. *et al.* 1994. The duration of zidovudine benefit in persons with asymptomatic HIV infection. *J. Amer. Med. Assoc.* **272**, 437–442.
Volberding, P. A. *et al.* 1990. Zidovudine in asymptomatic human immunodeficiency virus infection. *New England J. Med.* **322**, 941–949.
Wei, X. *et al.* 1995. Viral dynamics in human immunodeficiency virus type 1 infection. *Nature* **373**, 117–122.

Received 23 December 1996
Revised version accepted 4 March 1997